Brandstetter *et al.*
Egyptian Journal of Neurosurgery (2023) 38:22
https://doi.org/10.1186/s41984-023-00197-x

Egyptian Journal of Neurosurgery

RESEARCH Open Access

The foramen ovale: a keyhole to the brain? Computer simulations of percutaneous FO punctures

Maximilian Brandstetter[1,2,4*], Ammar Mallouhi[3] and François Alesch[1]

Abstract

Background The percutaneous cannulation of the foramen ovale (FO) is implemented in treating trigeminal neuralgia, diagnosing temporal lobe epilepsy and biopsy petroclival lesions. This study dealt with the question whether it is possible to reach intracerebral structures with a puncture beyond the Gasserian Ganglion (GG) without bone destruction or perforating vascularity.

Methods We considered the FO a natural keyhole and performed computer-simulated punctures through the right and left FO to eight intracerebral structures. Therefore, we took the Hartel and Submandibular (SM) approach as a starting point and planned trajectories with stereotactic planning software by using brain scans of ten patients.

Results The simulated punctures with the Hartel approach directly reached the hippocampus (20 out of 20 trajectories), the lateral ventricle (15/20) and the amygdala (2/20). The pons was reached (20/20); however, the pontine vascularity was within the course. The trajectories to the thalamus (13/20) ran through the hippocampus or the mesencephalon. The simulated punctures with the SM approach directly reached the amygdala (18/20), the lateral ventricle (5/20) and the putamen (20/20). The trajectories to the nucleus caudatus (20/20) pierced the hippocampus, the putamen or the maxillary artery. The courses to the thalamus (7/20) ran through the hippocampus or the mesencephalon. The sinus cavernosus could not be reached with the Hartel or SM approach.

Conclusions This study indicates that a percutaneous approach to the hippocampus, the lateral ventricle, the amygdala and the putamen is possible without harming major vessels or bone destruction. For a possible implementation of these trajectories in a clinical setting, it is necessary to prove these simulated punctures in cadaveric studies.

Keywords Anthropometric analysis, FO puncture, Keyhole neurosurgery, Trajectory, Brain surgery

Background

The FO is a bony defect with an average size of 7 × 4 mm in the sphenoid bone [1]. Hartel first described a percutaneous approach to the FO in 1914 [2]. Today this cannulation is implemented in the therapy of trigeminal neuralgia, the detection of epileptic seizures and punctures of local tumours in patients who cannot undergo open surgery due to comorbidity reasons. [3–5] The standard needle used for the puncture has a 20-gauge (diameter of 0,9 mm). [6].

The literature describes two percutaneous approaches to the FO: the Hartel approach and the SM approach [2,

*Correspondence:
Maximilian Brandstetter
max.brandstetter@live.at
[1] Neurosurgical Department, Medical University of Vienna, Waehringer Guertel 18-20, 1090 Vienna, Austria
[2] Department of Obstetrics and Gynecology, Paracelsus Medical University, Müllner Hautpstraße 48, 5020 Salzburg, Austria
[3] Radiological Department, Medical University of Vienna, Waehringer Guertel 18-20, 1090 Vienna, Austria
[4] Wilbrandtgasse 39, 1180 Vienna, Austria

6]. While the insertion point of the Hartel approach is 2,5—3 cm lateral to the oral commissure, the insertion point of the SM approach is medial to the mandibular angle [3, 6]. Consequently, Hartel's trajectory is parallel to a horizontal plane, which points towards the sensory root of the trigeminal nerve [6]. The plane of the submandibular approach is nearly parallel to a coronal plane pointed cephalad from the V3 to the V1 near the GG [6].

Morphometry plays an essential role in the misguided cannulations of the FO [1]. One factor is the FO's shape and size, which varies between ethical groups [7–9]. Another factor can be ossified ligaments of the inferior surface of the sphenoid bone, which exist close to the FO. They can occasionally be covered by osseous ligaments or compartmentalized by bony spurs [10–13]. In addition, the Foramen Versalius, a defect anomaly next to the FO, can cause misguidance [14].

The improvements in microsurgical techniques and diagnostic imaging allowed more minor approaches and resulted in the concept of keyhole neurosurgery. Since the 1980s, neurosurgeons have inserted miniature cameras and long, coaxial instruments into a tiny hole behind the ear and operated through a screen to minimize tissue disruptions and brain retraction [15, 16].

This study dealt with the question whether it is possible to reach intracerebral structures with an extended puncture beyond the GG without bone destruction or perforating vascularity. Considering the FO as a natural keyhole and taking the two standard percutaneous approaches as starting points, computer-simulated punctures to eight intracerebral structures were performed using brain scans of ten patients.

Material and methods

Patients

The CT- and MRI scans of ten patients treated in the Department of Neurosurgery of the Medical University Hospital of Vienna between November 2018 and November 2019 were included in this study. The inclusion criteria were that any neurological disease of the patient did not alter the anatomy of the skull and brain. The included indications were trigeminal neuralgia, preoperative planning of DBS electrodes and tumours of the cervical spine. Exclusion criteria in age and gender were not defined. (Table 1).

Table 1 The cohort of patients consisted of three females and seven males, all between 34 and 83 years of age. In six, the indication for undergoing imaging was trigeminal neuralgia; in three cervical spine tumours and one, the preoperative planning of DBS electrodes

	Age	Gender	Indication
Patient 1	50	Male	Trigeminal neuralgia
Patient 2	49	Male	DBS electrodes
Patient 3	51	Male	Meningeom C1
Patient 4	37	Female	Astrozytom C2
Patient 5	34	Male	Neurofibrom C2
Patient 6	57	Male	Trigeminal neuralgia
Patient 7	78	Female	Trigeminal neuralgia
Patient 8	83	Male	Trigeminal neuralgia
Patient 9	52	Male	Trigeminal neuralgia
Patient 10	72	Female	Trigeminal neuralgia

Imaging modalities

All images were performed with the standard radiological parameters according to the clinical indication. For this study, the used imaging modalities were a cCT with a bone window displaying the submandibular angle and a cMRI with T1 or T2 modality, performed with a 1,5 Tesla device.

Ethics

The patients' data were anonymized, and all procedures were performed following the ethical standards of the institutional and national research committee and with the 1964 Helsinki declaration and its later amendments or comparable ethical standards (Ethical commission of the Medical University of Vienna; No. 1902/2018).

Computer simulation

The identical patient's CT- and MRI scans were fused with stereotactic planning software.[1] The course of the two percutaneous approaches to the FO approach was taken as starting points for planning the trajectories. As shown in Fig. 1, the entry point of the Hartel approach is in the buccal area, and the course is consequently more flat-angled than in the SM approach [6].

Therefore, the Hartel approach was used to reach the hippocampus, the brainstem, the sinus cavernosus and the thalamus. The SM approach reached the amygdala, the putamen and the nucleus caudatus. The reaching of the ventricle was planned with both approaches. In each patient, the trajectories to the eight intracerebral structures were performed in the right and left of the skull. (Fig. 2).

[1] *Inomed Planning Software IPS 6: IPS* is a planning software used by neurosurgeons in stereotactic operations (e.g. biopsy or DBS) to plan a safe and precise approach.

Fig. 1 The probes display the extracranial course of the Hartel puncture (left) and the SM puncture (right)

Required parameters of the trajectories

The trajectory of each simulated FO puncture had to fulfil the following requirements (Fig. 3):

- Pass the FO
- Reach the target
- Avoid bone structures
- Avoid vital vascular structures
- The entry point had to be set at the skin

Definition of trajectories

With stereotactic planning, software trajectories were defined with an entry and a target point. In the Hartel approach, the standard entry point is 2,5—3 cm lateral to the angle of the mouth. [1] Comparable to the keyhole concept, the alteration of the entry point results in a change of trajectory course. A more medial intracerebral course resulted if the entry point was nearer to the mandibula. A definition next to the maxilla would result in a more lateral course. The inclination of the trajectory was defined through a more superior or inferior definition of the entry point. A superior entry point would result in a block by the petrosal part of the temporal bone.

The entry point was initially set in the axial plane of the CT scans, taking the further course of the trajectory into account (e.g. to reach the brainstem, a more lateral to medial path is necessary than to get to the hippocampus).

The SM approach's standard entry point is medial to the mandibular angle (20). A more medial intracerebral course resulted if the entry point was set next to the mandibula. A definition nearer to the pharynx resulted in a more lateral course. A change in a more anterior or posterior course was caused by a definition nearer to the anterior part of the mandibular or a more posterior entry next to the nearby running branches of the carotid artery.

The target point was set in the FO. The range is limited through the area of the FO of 7 mm × 4 mm. The position

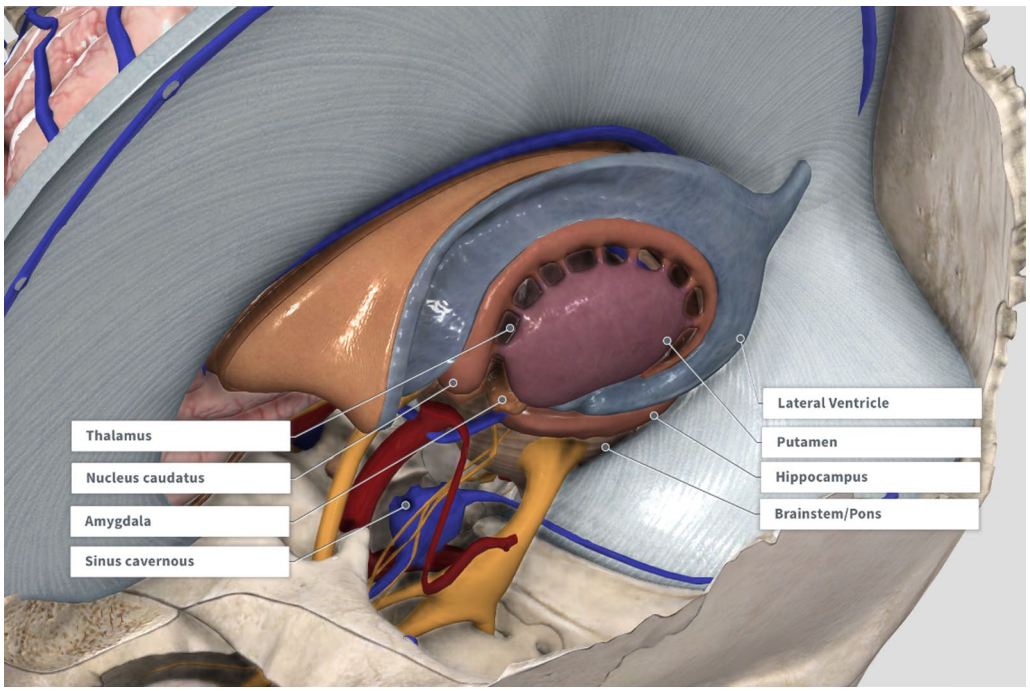

Fig. 2 Overview of the intracerebral target structures

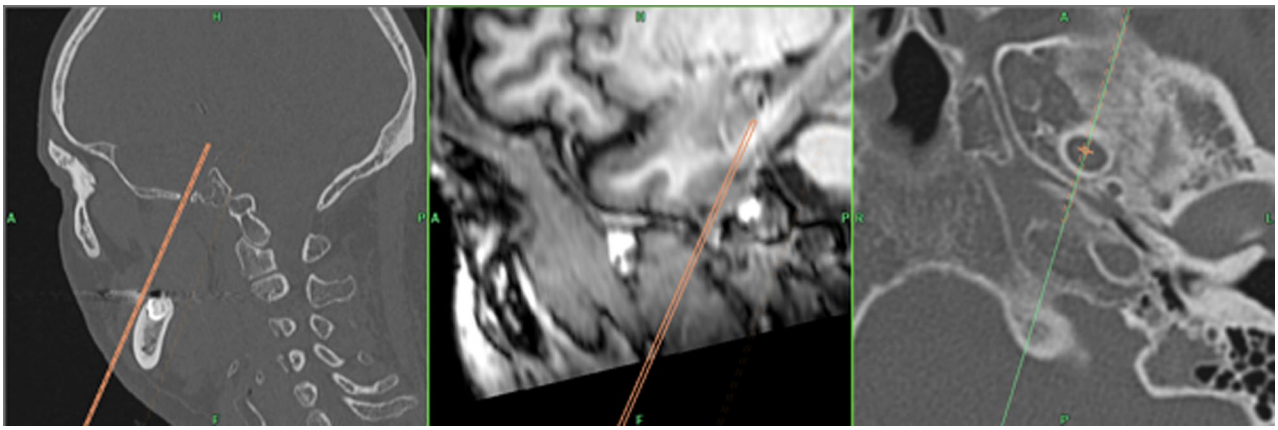

Fig. 3 Computer simulation to hippocampus fulfilling the required parameters

Table 2 List of trajectory measurements with explanation

Trajectory	
Measurement	**Description**
Length of trajectory	Distance between the entry point and target structure
Length of intracranial course	Distance between FO and the target structure
Height/sagittal angle	Angle between entry point, FO and the orbital floor (Hartel)/Point vertical to the FO next to the Entry point (SM)
Horizontal/coronal angle	Angle between Entry point, FO and inferior orbital ridge (Hartel)/Point vertical to the FO next to the Entry point (SM)
Entry point	In reference to a point at the center of the mouth, which was set at the intersection between the external surface of the lips and a sagittal plane through the dorsum sellae. (Hartel). In reference to a point which was set in the mandibular angle. (SM)

Table 3 List of measurements of the surrounding structures

Distances	
Vascularity	**Bones**
Maxillary artery	Maxilla
Internal carotid artery	Mandibula
Cerebri media artery	Pterygoid process
	Pars petrosus ossis temporalis (angle between trajectory and pars petrosus)

of the target point defines the trajectory in the following way: a more medial position of the target point in the FO results in a more medial intracerebral trajectory. Entry and target points were altered until the aimed intracerebral structure was reached through extrapolation of the course.

Measurements

As shown in Tables 2 and 3, the trajectory and distances to the surrounding structures were measured in each simulated puncture. Measurements of the trajectory and distances to passing bone structures were performed in the CT scans, while the distances to the passing soft tissue structures were performed in the MRI- scans (Fig. 4).

Statistical analysis

A summative trajectory for the right and left FO was measured for each target structure. Therefore, the mean and standard deviation of all ten patients were included. The statistical analysis was performed with a spreadsheet software.[2]

Results

Trajectories with the Hartel approach

The shortest trajectory in the Hartel approach was to the sinus cavernosus, while the longest was to the thalamus. The trajectory to the sinus cavernosus had the most lateral entry point, followed by the ones to the brainstem and the thalamus. These trajectories also had the biggest horizontal angle. The trajectories to these structures had a very medial to anterior course through the FO. The

[2] *Microsoft Excel software.*

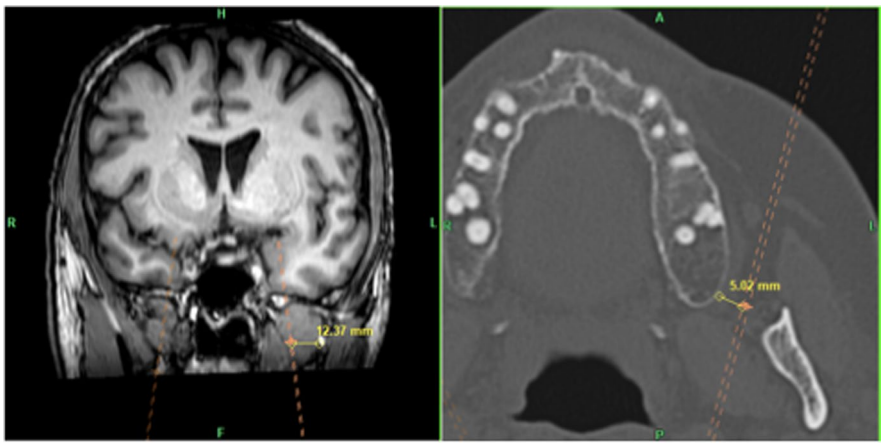

Fig. 4 MRI displays the distance of trajectory to the A. maxilaris, CT displays the distance to the maxilla

Table 4 Mean measurements of all Hartel trajectories (mm); TL = total length, EP = entry point (X/Y/Z), ALPHA = height angle, BETA = horizontal angle

	TL		EP		Alpha		Beta	
	Left	Right	Left	Right	Left	Right	Left	Right
Hippocampus	120.5	122.1	(42.4/30.5/26.9)	(38.8/34.8/29.6)	51.6	53.5	15.5	12.6
Ventricle	122.8	135.1	(42.7/30.7/26.6)	(37.1/28.7/29.1)	55.2	50.0	17.8	14.0
Brainstem	108.2	107.9	(57.8/36.2/10.2)	(52.7/35.4/12.0)	40.8	42.5	34.0	31.4
S. cavernosus	73.2	72.9	(73.9/75.3/18.2)	(71.4/71.7/19.0)	30.8	30.5	19.2	21.5
Amygdala	132.1	134.5	(50.4/48.0/25.7)	(39.4/38.3/21.0)	74.8	68.2	40.3	18.3
Thalamus	142.0	142.3	(53.3/42.4/19.4)	(45.0/35.1/23.1)	50.7	54.2	32.3	24.9

Table 5 Mean measurements of all Submandibular trajectories (mm); TL = total length, EP = entry point (X/Y/Z), SAGITTAL = sagittal angle, CORONAR = coronar angle

	TL		EP		Sagittal		Coronar	
	Left	Right	Left	Right	Left	Right	Left	Right
Ventricle	125.7	130.8	(16.4/31.2/49.5)	(16.8/35.6/46.2)	15.8	17.5	5.9	3.3
Amygdala	119.7	121.1	(10.6/27.5/40.4)	(9.2/19.8/39.1)	16.1	13.0	7.4	6.6
Putamen	153.3	157.7	(5.3/9.4/46.1)	(8.2/9.4/50.3)	7.7	7.4	9.6	7.6
N. caudatus	165.6	164.7	(5.9/8.5/46.0)	(7.1/8.6/48.1)	5.4	7.3	13.7	11.3
Thalamus	157.2	151.0	(4.0/23.0/42.7)	(5.2/30.6/38.0)	15.8	16.9	8.9	12.7

trajectories to the hippocampus and the lateral ventricle had the most medial entry points, with small horizontal angles and a very lateral approach through the FO. The steepest trajectory was the one to the lateral ventricle, followed by the one to the hippocampus and the thalamus. The flattest trajectories were the ones to the sinus cavernosus and the brainstem (Table 4).

Trajectories with SM approach

In the SM approach, the longest trajectory was the one to the nucleus caudatus, and the shortest was to the amygdala. The most anterior entry points were the ones to the lateral ventricle, followed by the thalamus and the amygdala. The trajectories to these structures also had the

biggest sagittal height angle. The most lateral entry points were the ones to the lateral ventricle and the amygdala. The courses to the amygdala and the nucleus caudatus had the biggest coronal angles. While the trajectory to the amygdala traversed the FO anteriorly, the trajectories to the thalamus traversed posteriorly. Putamen, nucleus caudatus and ventricle were reached via a lateral course through the FO. (Tables 5, 6).

Trajectories to structures

The measurements of the summative trajectories to all eight structures and an image of one trajectory to each structure are listed in the appendix.

The Hartel approach was used to reach the hippocampus in all ten patients. All defined trajectories fulfilled the postulated requirements on both sides. The target structure was always reached in the anterior part of the pes hippocampi. (Fig. 5, Table 7).

In seven patients, the Hartel approach was used on both sides to reach the lateral ventricle, while in two patients, the SM approach was used on both sides. There was one patient where the SM approach was used on the left side, and the Hartel approach was used on the right side. All trajectories fulfilled the postulated parameters (Figs. 6, 7, Tables 8, 9).

In nine patients, the SM approach was used to reach the amygdala. In one patient, the Hartel approach was used. All trajectories fulfilled the postulated requirements. The target structure was reached in the inferior part of the amygdala (Fig. 8, Table 10).

The SM approach was used in all ten patients to reach the putamen. All trajectories fulfilled the postulated requirements. The target structure was reached in the putamen's anterior and medial or lateral parts (Fig. 9, Table 11).

The Hartel approach was used to reach the brainstem in all ten patients. All trajectories did not fulfil the postulated requirements because the course ran next to or even through the pontine vascularity. The target structure was in the superior lateral part of the pons (Fig. 10, Table 12).

In all ten patients, the sinus cavernosus was reached with a trajectory, which ran between the process coronoideus and condylaris of the ramus mandibulae. The trajectories did not fulfil all the postulated requirements because neither the Hartel nor the SM approach could be used. The target structure was reached in the lateral part of the sinus cavernosus. (Fig. 11, Table 13).

The SubM approach was used in all ten patients to reach the nucleus caudatus. The trajectories did not fulfil all postulated requirements because a direct approach was impossible, and the putamen had to be pierced. In one patient, the middle cerebral artery was punctured. In two patients, the maxillary artery could not be identified. The target structure was reached in the anterior or lateral part of the nucleus caudatus (Fig. 12, Table 14).

The Hartel approach was used in seven patients on the left side to reach the thalamus, while the SM approach was used in three patients. On the right side, the Hartel approach was used in six patients and the SubM approach in four. The trajectories did not fulfil all postulated parameters because, within the course, the hippocampus and the mesencephalon were pierced (Figs. 13, 14, Tables 15, 16).

Discussion

This study dealt with the question whether it is possible to reach intracerebral structures beyond the GG, without bone destruction or perforating vascularity, by using an extended percutaneous approach to the FO. So far, the FO-cannulation has been implemented in the destructive therapy of trigeminal neuralgia, the detection of epileptic seizures with electrodes and punctures of tumours in the cavum Meckeli. [3, 4].

We considered the FO a natural keyhole and performed computer-simulated punctures to eight intracerebral structures. Therefore, we took the Hartel and SM approach as a starting point and planned trajectories with stereotactic planning software by using brain images of patients.

We showed that it is possible to reach the pes hippocampi directly with an adapted Hartel approach. This might also be of interest in taking biopsies of lesions in this area. Depending on the lesion's size and the trajectory's anatomical limitations, a keyhole transforaminal hippocampectomy might be an option. A course through the FO to the subarachnoid space around the hippocampus to get a better signal for an EEG is already being used in

Table 6 Key results

Target	Approach	Safety
Hippocampus	Hartel	Safe
Ventricle	Hartel + SM	Safe
Amygdala	SM	Safe
Putamen	SM	Safe
Brainstem	Hartel	Unsafe
Sinus cavernosus	Hartel	Unsafe
Nucleus caudatus	SM	Unsafe
Thalamus	Hartel + SM	Unsafe

the invasive diagnosis of temporal lobe epilepsy with the so-called FO-electrodes [4].

This study showed that reaching the lateral or the posterior horn of the lateral ventricle is possible with the Hartel and the SM approach. In the case of incarceration through hydrocephalus, a short and direct percutaneous ventricle puncture could save crucial seconds in contrast to a standard procedure of setting ventricle drainage.

The amygdala was reached through the FO with the SM approach. Due to the important role of the amygdala in the limbic system, there might be psychiatric indications for this trajectory in the future.

This study planned trajectories to the basal ganglia via the FO with the SM approach. It was possible to reach the putamen directly. A course of the trajectories to the nucleus caudatus pierced other intracerebral structures, primarily the putamen. As the basal ganglia play an essential role in the extrapyramidal motoric system and consequently in moving disorders, they are potential targets in surgical treatments, like deep brain stimulation. Due to the safety of the standard approach through the parietal skull, a transforaminal insertion of deep brain electrodes to reach the basal ganglia is not likely.

The trajectories to the brainstem ran closely or even through the posterior circulation vessels, which would be too dangerous to be realized in a clinical setting. In individual scenarios, a puncture of brainstem lesions could be an option but only guided with neuronavigation and a stereotactic frame.

We planned trajectories through the FO to reach the sinus cavernosus with the idea of taking biopsies of nearby lesions. However, the course must be considered critically because of its lateral entry point. The clinical relevance of a percutaneous puncture of the sinus cavernosus must be regarded critically. The closeness to vital anatomical structures, especially the internal carotid artery, makes the trajectory risky, and any deviation from the course could lead to severe bleeding.

The thalamus could not be reached without piercing other structures, such as the hippocampus or the mesencephalon. As the thalamus has a crucial function in perception, any damage would severely affect the quality of a patient's life. What might be a clinical implementation is the biopsy of lesions in the area of the thalamus. The nucleus subthalamicus or other nuclei of the thalamus were not able to be differentiated with the used MRI scans.

Limitations

One limitation of this study is the limited cohort of only ten patients. Secondly, the quality of the CT and MRI scans had to be collected in a clinical setting. The third limitation is the omission of cadaveric studies.

Conclusions

This study indicates that a transforaminal and percutaneous approach to the hippocampus, the lateral ventricle, the amygdala and the putamen is possible without harming major vessels or bone destruction. For a possible implementation of these trajectories in a clinical setting, it is necessary to prove these simulated punctures in cadaveric studies.

Appendix

See Figs. 5, 6, 7, 8, 9, 10, 11, 12, 13, 14
See Tables 7, 8, 9, 10, 11, 12, 13, 14, 15, 16.

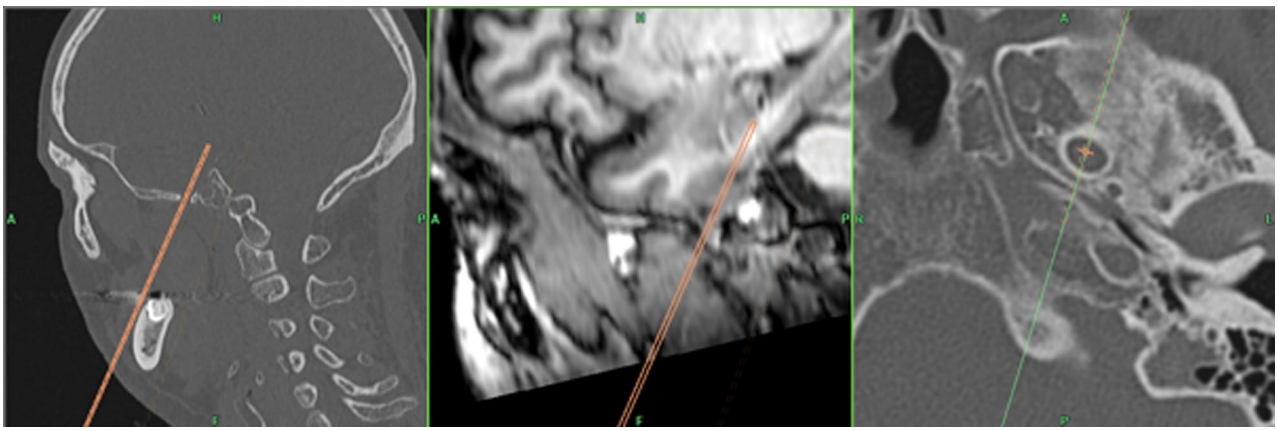

Fig. 5 Hartel approach to Hippocampus

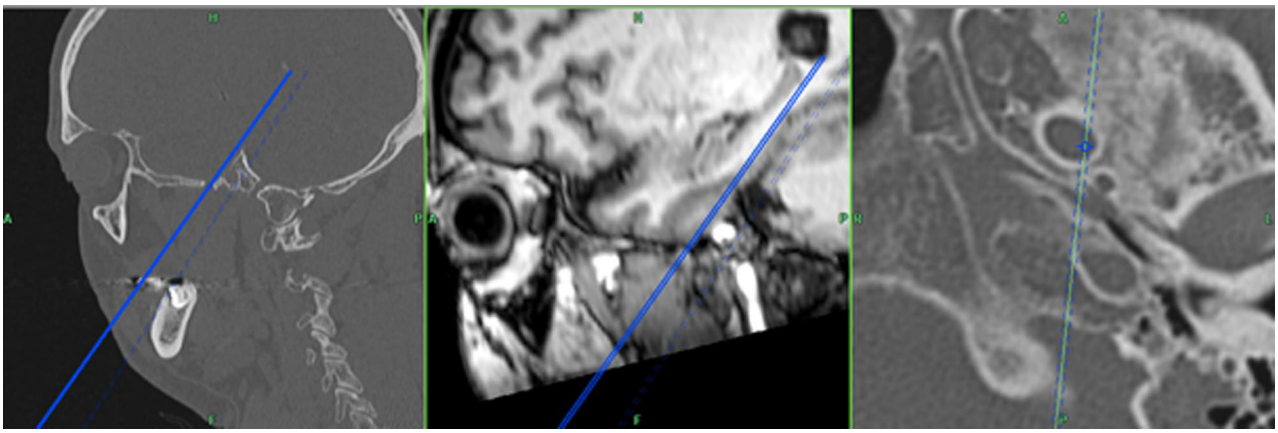

Fig. 6 Hartel approach to the lateral ventricle

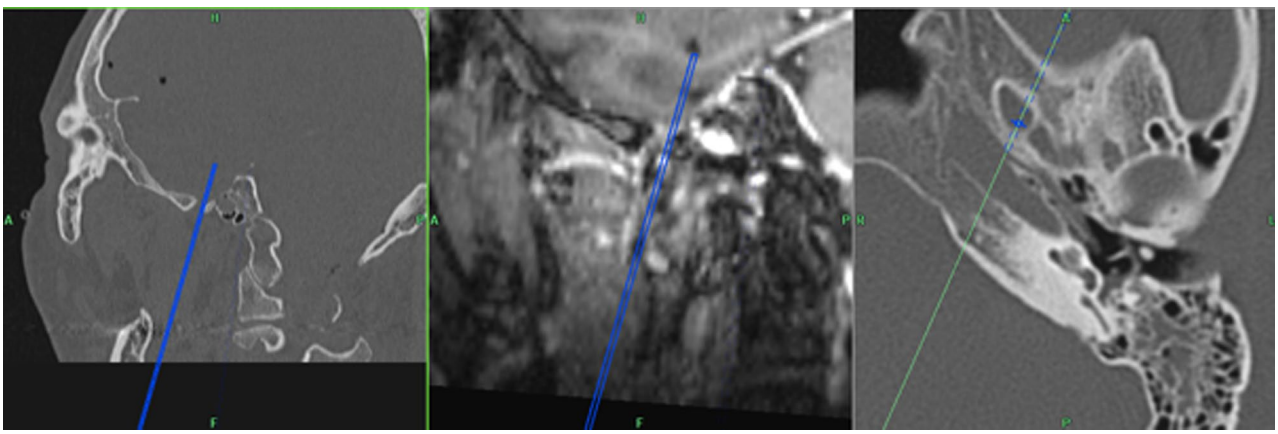

Fig. 7 SM approach to the lateral ventricle

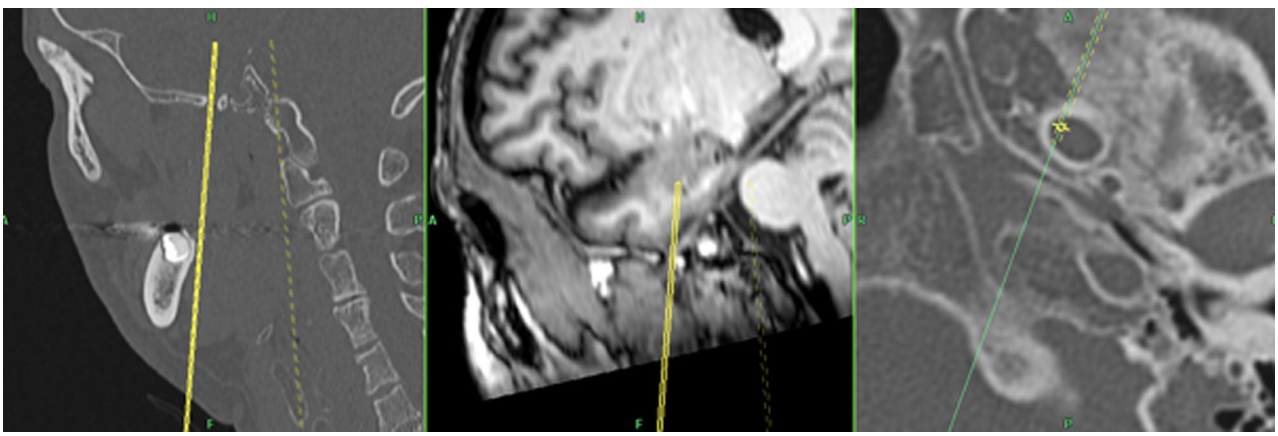

Fig. 8 SM approach to Amygdala

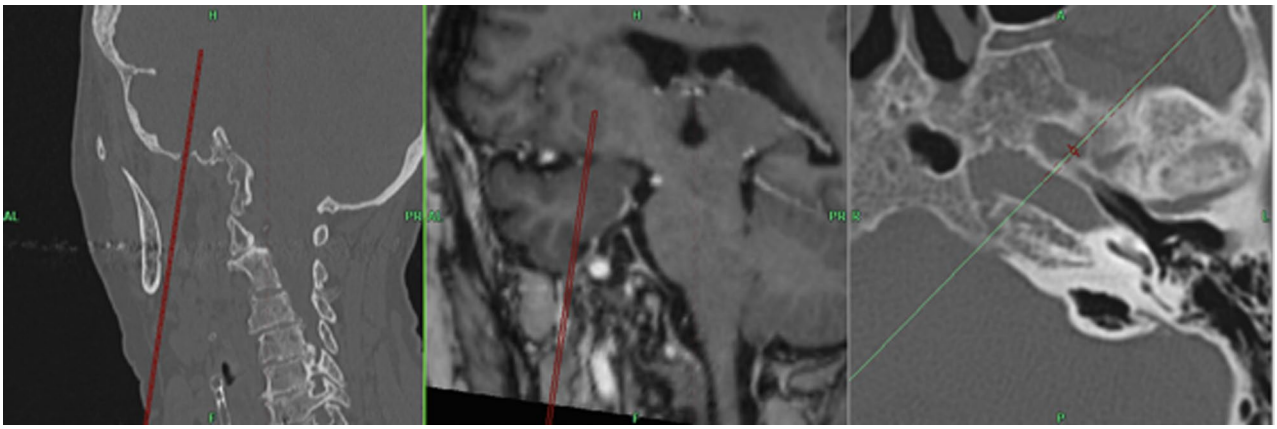

Fig. 9 SM approach to Putamen

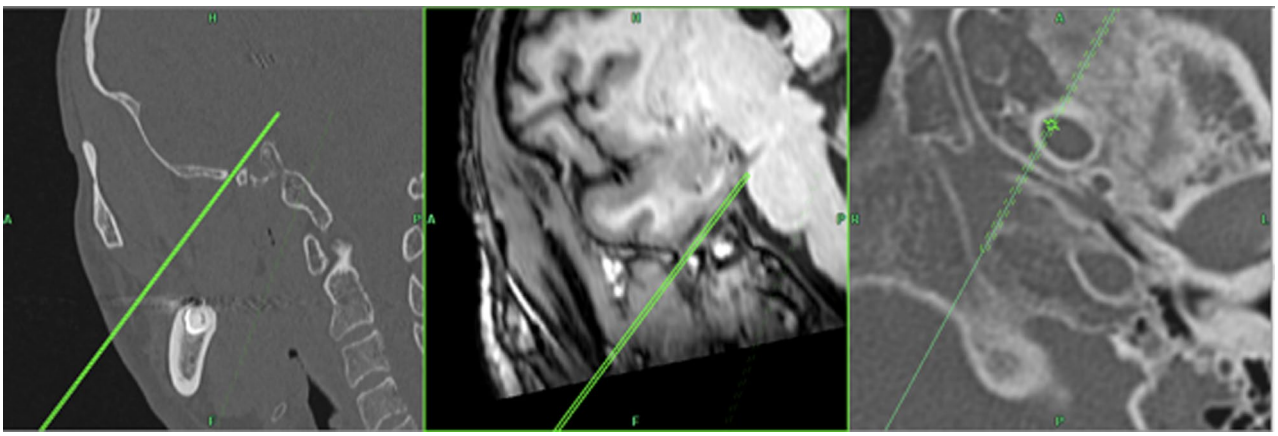

Fig. 10 Hartel approach to Brainstem

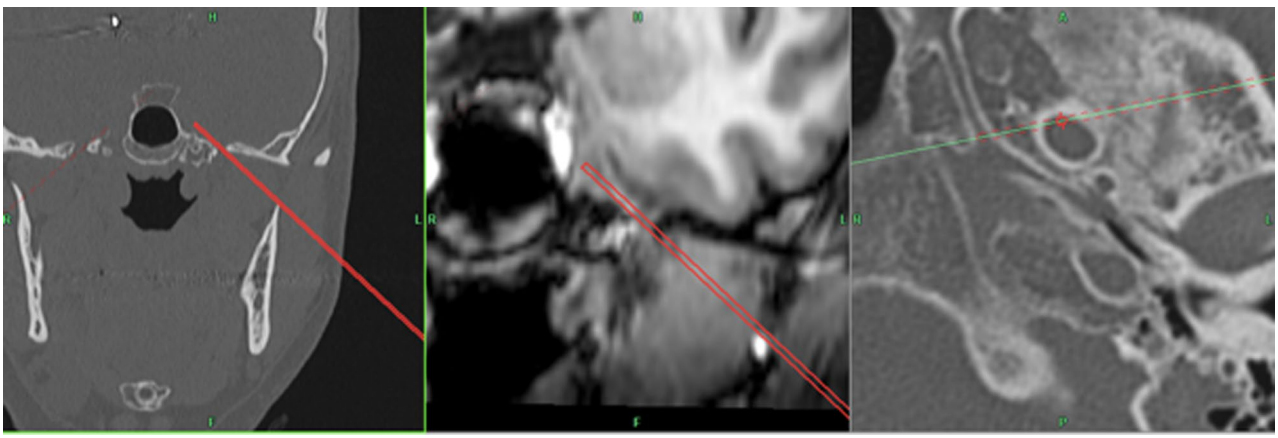

Fig. 11 Hartel approach to Sinus cavernosus

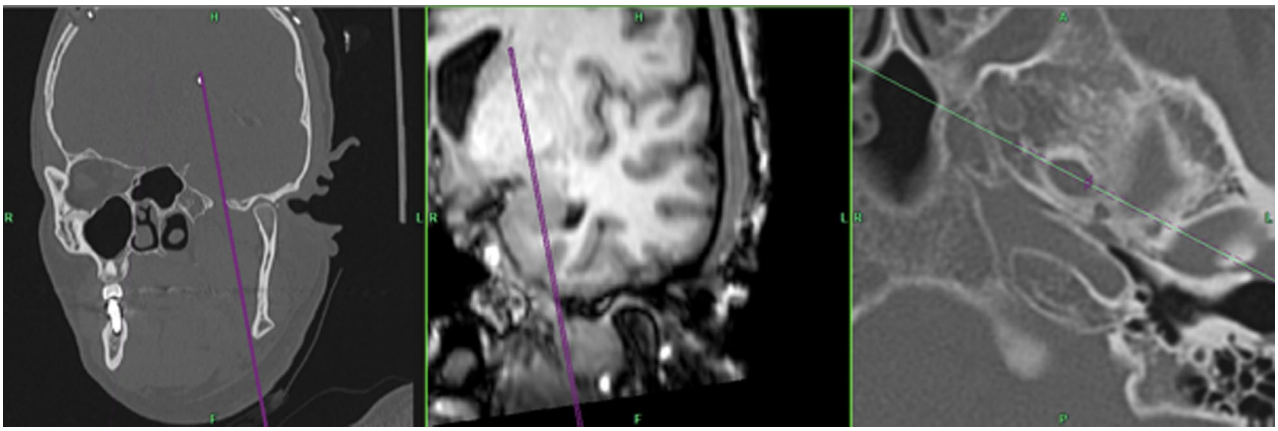

Fig. 12 SM approach to Nucleus caudatus

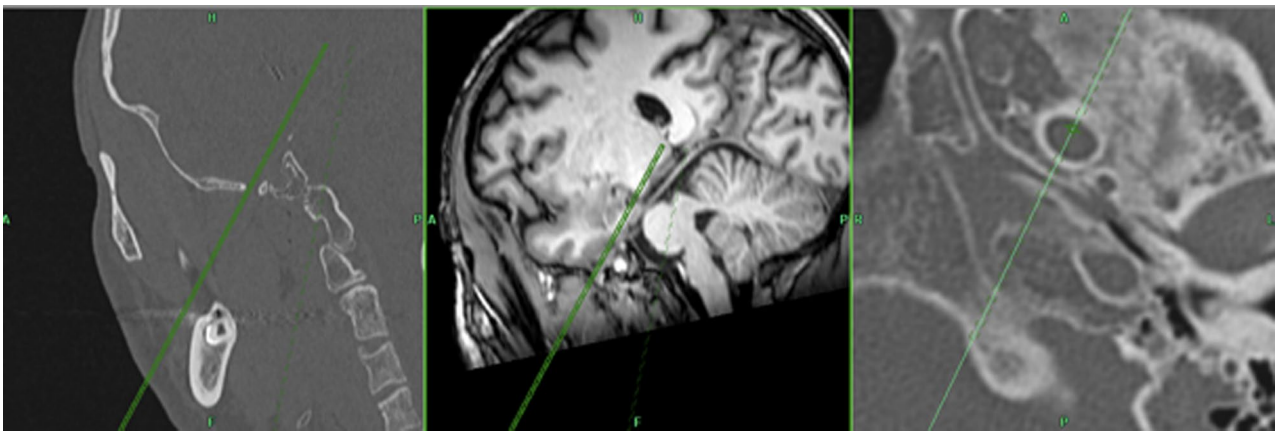

Fig. 13 Hartel approach to the thalamus

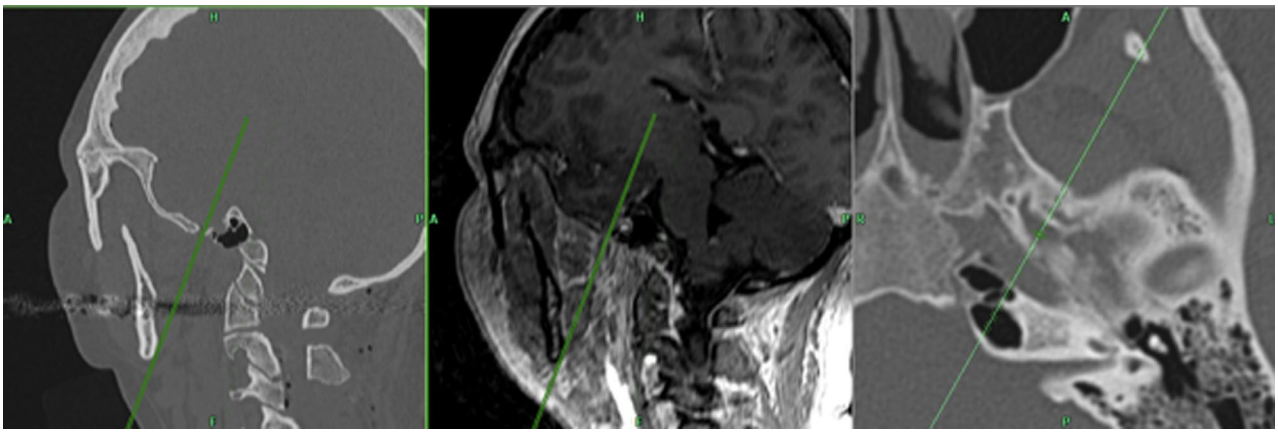

Fig. 14 SM approach to the thalamus

Table 7 Mean measurements of trajectory to hippocampus (mm)

	Hippocampus	
Access	**Hartel**	
Side	**Left**	**Right**
Number	10	10
FO	Lateral	Lateral
TL	120.5 (±10,5)	122.1 (± 11.3)
ICL	26.1 (± 2.4)	26.8 (±4.4)
ALPHA	51.6° (± 7.9°)	53.5° (±7.6°)
BETA	15.5° (±7.6°)	12.6° (±6.6°)
Maxilla	4.9 (±2.0)	6.7 (±3.0)
Mandibula	7.4 (±2.3)	5.3 (±3.1)
Pterygoid	4.0 (±1.9)	3.6 (±1.0)
Pars petrosus	19.8° (±5.6)	17.7° (±4.4)
A. maxillaris	12.5 (±3.8)	11.7 (±4.9)
A. carotis	8.2 (± 2.9)	9.2 (± 1.6)

FO = position of trajectory in foramen ovale, TL = total length of trajectory, ICL = intra cranial length, Alpha = height angle, BETA = horizontal angle

Table 8 Mean measurements of Hartel approach to the ventricle (mm)

	Ventricle	
Access	**SubM**	
Side	**Left**	**Right**
Number	3	2
FO	Posterolateral	Posterolateral
TL	122.8 (± 18.0)	135.1 (±23.8)
ICL	32.7 (±20.0)	42.6 (±20.9)
Alpha	55.2° (±10.9°)	50.0° (±9.8°)
BETA	17.8° (±11.4°)	14.0° (±8.3°)
Maxilla	5.5 (±3.2)	5.2 (±4.4)
Mandibula	6.1 (±2.7)	6.4 (±4.7)
Pterygoid	4.9 (±3.3)	4.5 (±0.6)
Pars petrosus	20.2 (±8.1)	13.3 (±9.4)
A. maxilaris	9.8 (±4.9)	12.6 (±8.6)
A. carotis	8.5 (±3.0)	9.2 (±2.2)

FO = position of trajectory in foramen ovale, TL = total length of trajectory, ICL = intra cranial length, ALPHA = height angle, BETA = horizontal angle

Table 9 Mean measurements of SM approach to ventricle (mm);

	Ventricle	
Access	**SubM**	
Side	**Left**	**Right**
Number	3	2
FO	Posterolateral	Posterolateral
TL	125.7 (±6,1)	130,8(±0,9)
ICL	17,9 (±3,8)	20,3 (±1,3)
SAGITTAL	15,8° (±8,5°)	17,5° (±10,4°)
CORONAR	5,9° (±9,6°)	3,3° (±3,5°)
Mandibula	9,2 (±6,8)	7,5 (±1,3)
Pterygoid	5,4 (±2,2)	5,4 (±0,7)
Pars petrosus	34,9° (±6,1)	30,1° (±10,0)
A. maxilaris	13,8 (±3,6)	6,2 (±6,1)
A. carotis	11,1 (±4,1)	8,8 (±0,0)

FO = position of trajectory in foramen ovale, TL = total length of trajectory, ICL = intra cranial length, SAGITTAL = sagittal angle, CORONAR = coronar angle

Table 10 Mean measurements of trajectory to amygdala (mm)

	AMYGDALA	
Access	**SubM**	
Side	**Left**	**Right**
Number	9	9
FO	Indefinite	Indefinite
TL	119.7 (± 7.4)	121.1 (± 12.0)
ICL	21.3 (± 1.5)	23.5 (± 2.7)
SAGITTAL	16.1° (± 6.1°)	13.0° (± 6.2°)
CORONAR	7.4° (± 5.3°)	6.6° (± 4.4°)
Mandibula	3.7 (± 2.6)	4.9 (± 3.7)
Pterygoid	6.0 (± 4.0)	6.9 (± 3.5)
Pars petrosus	40.1° (± 6.0)	37.8° (± 4.9)
A. maxilaris	8.8 (± 6.7)	11.2 (± 7.4)
A. carotis	10.4 (± 1.8)	10.0 (± 2.4)

FO = position of trajectory in foramen ovale, TL = total length of trajectory, ICL = intra cranial length, SAGITTAL = sagittal angle, CORONAR = coronar angle

Table 11 Mean measurements of trajectory to putamen (mm)

	PUTAMEN	
Access	**SubM**	
Side	**LEFT**	**RIGHT**
Number	10	10
FO	Lateral	Lateral
TL	153.3 (± 18.3)	157.7 (± 16.6)
ICL	43.2 (± 4.5)	45.6 (± 6.2)
SAGITTAL	7.7° (± 5.9°)	7.4° (± 2.5°)
CORONAR	9.6° (± 5.3°)	7.6° (± 4.7°)
Mandibula	7.1 (± 2.2)	8.2 (± 4.7)
Pterygoid	9.0 (± 3.8)	9.0 (± 4.7)
Pars petrosus	55.0° (± 9.3)	43.9° (± 16.5)
A. maxilaris	8.1(± 4.8)	8.1 (± 5.7)
A. carotis	11.8 (± 2.5)	11.0 (± 2.1)
A.cer.med	4.7 (± 3.5)	5.2 (± 4.3)

FO = position of trajectory in foramen ovale, TL = total length of trajectory, ICL = intra cranial length, SAGITTAL = height angle, CORONAR = coronar angle, A.cer.med = cerebrimed

Table 12 Mean measurements of trajectory to brainstem (mm)

	BRAINSTEM	
Access	**Hartel**	
Side	**LEFT**	**RIGHT**
Number	10	10
FO	Anterior	Anterior
TL	108.2 (± 7.9)	107.9 (± 8.9)
ICL	31.6 (± 2.8)	30.9 (± 3.1)
ALPHA	40.8° (± 7.6°)	42.5° (± 5.9°)
BETA	34.0° (± 7.3°)	31.4° (± 8.4°)
Maxilla	13.0 (± 3.0)	11.1° (± 2.0)
Mandibula	0.8 (± 0.3)	2.0 (± 1.5)
Pterygoid	9.1 (± 2.1)	7.4 (± 1.8)
Pars petrosus	7.5° (± 4.9)	7.6° (± 3.5)
A. maxilaris	8.4 (± 3.6)	10.2 (± 8.2)
A. carotis	4.7 (± 2.0)	6.0 (± 2.0)

FO = position of trajectory in foramen ovale, TL = total length of trajectory, ICL = intra cranial length, ALPHA = height angle, BETA = horizontal angle

Table 13 Mean measurements of trajectory to Sinus cavernosus (mm)

	SINUS CAVERNOSUS	
Access	**Hartel**	
Side	**LEFT**	**RIGHT**
Number	10	10
FO	anterior	anterior
TL	73.2 (± 12.7)	72.9 (± 9.9)
ICL	8.7 (± 3.8)	10.0 (± 4.6)
ALPHA	30.8° (± 11.4°)	30.5° (± 10.4°)
BETA	19.2° (± 17.6°)	21.5° (± 18.7°)
Mandibula	1.0 (± 0.6)	1.0 (± 0.4)
A. maxilaris	9.6 (± 5.2)	9.6 (± 6.9)
A. carotis	5.4 (± 5.2)	3.7 (± 2.8)

FO = position of trajectory in foramen ovale, TL = total length of trajectory, ICL = intra cranial length, ALPHA = height angle, BETA = horizontal angle

Table 14 Mean measurements of trajectory to putamen (mm)

	Nucleus caudatus	
Access	**SubM**	
Side	**LEFT**	**RIGHT**
Number	10	10
FO	Anterolateral	Posterior
TL	165.6 (± 18.9)	164.7 (± 20.5)
ICL	56.5 (± 8.4)	57.2 (± 7.3)
SAGITTAL	5.4° (± 3.3°)	7.3° (± 3.7°)
CORONAR	13.7° (± 4.8°)	11.3° (± 5.0°)
Mandibula	3.4 (± 3.7)	4.4 (± 4.6)
Pterygoid	7.8(± 4.3)	8.4 (± 4.3)
Petrosus	51.9 (± 8.6)	47.6 (± 7.4)
A. maxilaris	6.7 (± 4.7)	8.9 (± 4.2)
A. carotis	10.0 (± 2.6)	8.9 (± 2.6)
A.cer.med	3.4 (± 3.3)	2.5 (± 2.0)

FO = position of trajectory in foramen ovale, TL = total length of trajectory, ICL = intra cranial length, SAGITTAL = height angle, CORONAR = coronar angle, A.cer.med = cerebri media

Table 15 Mean measurements of trajectory to thalamus (mm)

	THALAMUS	
Access	**Hartel**	
Side	**Left**	**Right**
Number	7	6
FO	Anterolateral	Indefinite
TL	142.0 (± 8.3)	142.3 (± 11.6)
ICl	53.8 (± 3.4)	53.9 (± 3.8)
ALPHA	50.7° (± 13.6°)	54.2° (± 14.0°)
BETA	32.3° (± 11.5°)	24.9° (± 14.2°)
Maxilla	11.4 (± 1.7)	8.8 (± 2.0)
Mandibula	1.8 (± 0.9)	3.5 (± 3.0)
Pterygoid	7.1 (± 2.3)	4.0 (± 2.1)
Petrosus	26.0 (± 5.9)	21.6 (± 5.8)
A. maxilaris	9.2 (± 2.1)	10.2 (± 8.4)
A. carotis	8.4 (± 1.6)	7.8 (± 2.8)
A.cer.med	9.2 (± 6.9)	12.1 (± 7.5)

FO = position of trajectory in foramen ovale, TL = total length of trajectory, ICL = intra cranial length, SAGITTAL = height angle, CORONAR = coronar angle, A.cer.med = cerebri med

Table 16 Mean measurements of trajectory to thalamus (mm)

	THALAMUS	
Access	**SubM**	
Side	**Left**	**Right**
Number	3	4
FO	Posterior	Indefinite
TL	157.2 (± 17.9)	150.8 (± 23.1)
ICL	52.5 (± 3.6)	48.1 (± 5.4)
SAGITTAL	15.8° (± 2.9°)	16.7° (± 6.7°)
CORONAR	8.9° (± 5.3°)	12.7° (± 4.2°)
Mandibula	3.3 (± 4.2)	2.1 (± 1.7)
Pterygoid	7.8 (± 1.4)	6.5 (± 3.7)
Petrosus	34.5 (± 4.0)	34.1 (± 4.8)
A. maxilaris	11.5 (± 4.4)	12.4 (± 2.6)
A. carotis	10.0 (± 3.8)	8.9 (± 1.3)
A.cer.med	8.7 (± 0.7)	8.0 (± 5.3)

FO = position of trajectory in foramen ovale, TL = total length of trajectory, ICL = intra cranial length, SAGITTAL = height angle, CORONAR = coronar angle, A.cer.med = cerebri med

Abbreviations

A	Artery
CT	Computed tomography
DBS	Deep brain stimulation
EEG	Electroencephalography
EP	Entry point
FO	Foramen ovale
GG	Gasserian Ganglion
ICL	Intra cranial length
IPS	Inomed Planning Software
MRI	Magnetic resonance imaging
SM	Submandibular
TL	Total length
V1	Ophthalmic nerve
V3	Mandibular nerve

Acknowledgements
The authors thank Mrs Dengler, product management of Inomed, and Mr Dengler, Sales Director of Inomed, for providing the planning software IPS6.

Author contributions
MB performed the trajectory measurements and was a major contributor to writing the manuscript. FA was responsible for conceptualization, methodology, formal analysis of the paper and reviewing the manuscript. AM analyzed and interpreted the radiologic images and trajectories. All authors read and approved the final manuscript.

Funding
No funding was received for this research.

Availability of data and materials
The datasets used and analyzed during this study are available from the corresponding author upon reasonable request.

Declarations

Ethics approval
All procedures involving human participants in this study followed the institutional and national research committee's ethical standards, the 1964 Helsinki declaration, and its later amendments or comparable ethical standards. (Ethical commission of the Medical University of Vienna; No. 1902/2018).

Consent for publication
Not applicable, as data were analyzed retrospectively and anonymously.

Competing interests
All authors certify that they have no affiliations with or involvement in any organization or entity with any financial interest (such as honoraria; educational grants; participation in speakers' bureaus; membership, employment, consultancies, stock ownership, or other equity interest; and expert testimony or patent-licensing arrangements), or non-financial interest (such as personal or professional relationships, affiliations, knowledge or beliefs) in the subject matter or materials discussed in this manuscript.

Received: 5 September 2022 Accepted: 30 January 2023
Published online: 01 May 2023

References

1. Zdilla MJ, Fijalkowski KM. The shape of the foramen ovale: a visualization aid for cannulation procedures. J Craniofac Surg. 2017;28(2):548–51.
2. Peris-Celda M, Graziano F, Russo V, Mericle RA, Ulm AJ. Foramen ovale puncture, lesioning accuracy, and avoiding complications: microsurgical anatomy study with clinical implications. J Neurosurg. 2013;119(5):1176–93.
3. Shane Tubbs R, J Dixon, Marios Loukas, Aaron A. Cohen-Gadol. Regional vascular relationships to the foramen ovale: an anatomical study with application to approaches to the external skull base with an emphasis on transcutaneous procedures for the treatment of trigeminal neuralgia. J Neurosurg. 2010;113(3):493–7.
4. Sheth SA, Aronson JP, Shafi MM, Phillips HW, Velez-Ruiz N, Walcott BP, et al. Utility of foramen ovale electrodes in mesial temporal lobe epilepsy. Epilepsia. 2014;55(5):713–24.
5. Arishima H, Kawajiri S, Arai H, Higashino Y, Kodera T, Kikuta K. Percutaneous glycerol rhizotomy for trigeminal neuralgia using a single-plane, flat panel detector angiography system: technical note. Neurol Med Chir. 2016;56(5):257–63.

6. Ding W, Chen S, Wang R, Cai J, Cheng Y, Yu L, et al. Percutaneous radiofrequency thermocoagulation for trigeminal neuralgia using neuronavigation-guided puncture from a mandibular angle. Medicine. 2016;95(40).
7. Zdilla MJ, Hatfield SA, McLean KA, Laslo JM, Cyrus LM, Lambert HW. Orientation of the foramen ovale: an anatomic study with neurosurgical considerations. J Craniofac Surg. 2016;27(1):234–7.
8. Somesh MS, Sridevi HB, Prabhu LV, Swamy MS, Krishnamurthy A, Murlimanju BV, et al. A morphometric study of foramen ovale. Turk Neurosurg. 2011;21(3):378–83.
9. Patil J, Kumar N, KG MR, Nayak S, Marpalli S, Ashwini LS. The foramen ovale morphometry of sphenoid bone in South Indian population. J Clin Diagnost Res JCDR. 2013;7(12):2668–70.
10. Natsis K, Piagkou M, Skotsimara G, Totlis T, Apostolidis S, Panagiotopoulos NA, et al. The ossified pterygoalar ligament: an anatomical study with pathological and surgical implications. J Cranio-Maxillo-Fac Surg. 2014;42(5):e266–70.
11. Ryu S-JJ, Park M-KK, Lee UYY, Kwak H-HH. Incidence of pterygospinous and pterygoalar bridges in dried skulls of Koreans. Anatomy Cell Biol. 2016;49(2):143–50.
12. Tubbs RS, May WR, Apaydin N, Shoja MM, Shokouhi G, Loukas M, et al. Ossification of ligaments near the foramen ovale: an anatomic study with potential clinical significance regarding transcutaneous approaches to the skull base. Neurosurgery. 2009;65(6 Suppl):60.
13. Pekala PA, Henry BM, Pekala JR, Fraczek PA, Taterra D, Natsis K, et al. The pterygoalar bar: a meta-analysis of its prevalence, morphology and morphometry. J Cranio-Maxillo-Facial Surg. 2017;45(9):1535–41.
14. Chaisuksunt V, Kwathai L, Namonta K, Rungruang T, Apinhasmit W, Chompoopong S. Occurrence of the foramen of Vesalius and its morphometry relevant to clinical consideration. Scientific World J. 2012;2012: 817454.
15. Reisch R, Stadie A, Kockro RA, Hopf N. The keyhole concept in neurosurgery. World Neurosurg. 2013;79(2 Suppl):S17.e9–3.
16. Amirjamshidi A. Key hole craniotomy: when, where, and how to apply? Asian J Neurosurg. 2019;14(3):619–20.

Publisher's Note